Available online at www.sciencedirect.com
SCIENCE DIRECT®

ELSEVIER

Solid State Communications 135 (2005) 179–182

solid state communications

www.elsevier.com/locate/ssc

The structural and optical properties of ZnO nanorod arrays

X.Q. Meng[a,b], D.Z. Shen[a,*], J.Y. Zhang[a], D.X. Zhao[a], Y.M. Lu[a], L. Dong[a,b], Z.Z. Zhang[a], Y.C. Liu[c], X.W. Fan[a]

[a]*Key Laboratory of Excited State Processes, Changchun Institute of Optics, Fine Mechanics and Physics, Chinese Academy of Sciences, 16 East Nan-Hu Road, Open Economic Zone, Changchun 130033, People's Republic of China*
[b]*Graduate School of the Chinese Academy of Sciences, People's Republic of China*
[c]*Center for Advanced Optoelectronic Functional Material Research, Northeast Normal University, Changchun 130024, People's Republic of China*

Received 30 October 2004; accepted 15 April 2005 by R. Merlin

Abstract

High quality vertical-aligned ZnO nanorod arrays were synthesized by a simple vapor transport process on Si (111) substrate at a low temperature of 520 °C. Field-emission scanning electron microscopy (FESEM) showed the nanorods have a uniform length of about 1 μm with diameters of 40–120 nm. X-ray diffraction (XRD) analysis confirmed that the nanorods are *c*-axis orientated. Selected area electron diffraction (SAED) analysis demonstrated the individual nanorod is single crystal. Photoluminescence (PL) measurements were adopted to analyze the optical properties of the nanorods both a strong UV emission and a weak deep-level emission were observed. The optical properties of the samples were also tested after annealing in oxygen atmosphere under different temperatures, deep-level related emission was found disappeared at 600 °C. The dependence of the optical properties on the annealing temperatures was also discussed.

PACS: 73.61.Tm; 78.66.−w; 81.05.Dz

Keywords: A. Nanorods; D. Optical properties; C. Scanning and transmission electron microscopy

1. Introduction

In recent years, the synthesis and characterization of one-dimensional (1D) semiconductor nanostructures have attracted much interest, because of their unique and fascinating optical, electrical, mechanical and thermo-electrical properties and potential technology applications. Nanodevices based on 1D semiconductors have been used in the realm of field-effect switch [1], single electron transistor [2], biological and chemical sensors [3] and light-emitting devices [4]. Among various nanostructured materials, ZnO is particular important due to its wide band-gap (3.37 eV) and large binding energy (60 meV) [5]. One of the representative 1D ZnO nanostructures is nanorods. Up to now, many methods have been accomplished for preparing ZnO nanorods, including physical vapor deposition [6], vapor phase transport [7–9], chemical vapor deposition [10,11], surfactant assisted hydrothermal method [12,13], and soft solution method [14]. The preparation of well-aligned high quality ZnO nanorod arrays with uniform length and controlled nucleation at low temperature is still desired, for well-aligned ZnO nanorod arrays can be used to fabricate ZnO nanorods Schottky diode [15] and ZnO based nanorod heterojunctions [16–18].

In this letter, we synthesized high quality ZnO nanorod arrays on Si (111) substrate at a low temperature of 520 °C by simple vapor phase transport method. The structural and optical

---

* Corresponding author. Tel.: +86 4316176322; fax: +86 4314627031.
E-mail address: meng_xiuqing@yahoo.com.cn (D.Z. Shen).

0038-1098/$ - see front matter © 2005 Elsevier Ltd. All rights reserved.
doi:10.1016/j.ssc.2005.04.015

properties were analyzed. The dependence of the optical properties on the annealing temperatures was also discussed.

2. Experimental details

The material growth was carried out in a traditional horizontal furnace by a simple vapor phase transport process. Zinc powder (99.99%) was loaded into a quartz boat in the center of the furnace and served as the source. Si (111) substrate pre-coated with a thin layer (about 2 nm) of Au catalyst was laid above the zinc source with a distance of 4mm. The furnace was then ramped to 520 °C under a constant flow (300 sccm) of pure Ar gas. After the desired temperature was reached, pure Ar gas was switched to nitrogen gas to start the ZnO growth. The oxygen source was unintentionally introduced by the residual O_2 components in the nitrogen gas. After specific growth period, nitrogen gas was switched back to pure Ar gas and the furnace was stopped heating. The surface of the sample presented a white gray colored layer after cooled down and taken out of the furnace. The as-synthesized material was then analyzed by the field-emission scanning electron microscopy (FESEM), energy-dispersive X-ray spectroscopy (EDX) attached to SEM, transmission electron microscopy (TEM), X-ray diffraction (XRD), Raman scattering, and PL measurement.

3. Results and discussion

Fig. 1 shows the FESEM image of the nanorod arrays grown on Si (111) substrate at 520 °C for 20 min. In the FESEM image, high-density well-aligned hexagonal shaped ZnO nanorods were perpendicularly pointing out of the substrate. The nanorods have a uniform length of about 1 μm with diameters ranging from 40 to 120 nm. But for each nanorod, it shows an even diameter from the top to the bottom. The enlarged FESEM image in the inset of Fig. 1 further indicates the shape of the rod is hexagonal and the surface of its top is flat. The average distribution of the ZnO nanorods on substrate is about 3.2×10^{13} m^2. EDX result shows that the nanorods consist of zinc and oxygen elements only (figure is not given). Although we used Au as catalyst, there is no signal of catalyst particles from the analyses of FESEM and EDX. The absence of Au catalyst in the observation of FESEM and EDX has been reported previously [19,20].

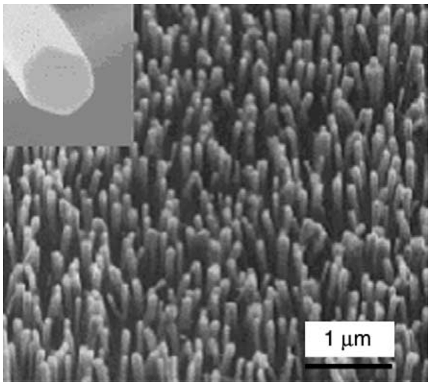

Fig. 1. SEM image of the ZnO nanorod arrays. The inset is the top view of enlarged FESEM image of a ZnO nanorod.

Fig. 2 shows the X-ray diffraction pattern of ZnO nanorod arrays. We can see only one diffractive peak besides the diffraction peak of Si (111) substrate in the pattern, which belongs to ZnO wurtzite structure. No diffraction peak of Zn or other phase was observed. The full width at half maximum (FWHM) of sharp (002) diffraction peak is only 0.21°, which indicates the nanorods growth is c axial orientation, in accord with the FESEM result. To our knowledge, such an excellent XRD result of ZnO nanorods synthesized by this kind of simple method was not reported yet.

TEM image of the single nanorod is shown in Fig. 3. As testified, the nanorod is straight and its sidewalls are smooth. The nanorod diameter is uniform from the top to the bottom. SAED analysis indicates that the nanorod is a single-crystal with a growth direction along *c*-axis, as shown in the inset of Fig. 3, which verifies the XRD result.

Fig. 4 demonstrates the Raman spectrum of the ZnO nanorods. The peak at 438 cm^{-1} is attributed to E_2 (high) mode and the peak at 579 cm^{-1} is A_1 (LO) mode at low wave number region. Compared with bulk material the E_2 (high) mode and A_1 (LO) mode show 1 and 5 cm^{-1} blueshift, respectively [21]. Two reasons may be responsible for the blue shift: one is due to the broken of symmetry in nanocrystals, which lead the original prohibited transformation to allowed transmission, correspondingly some new peaks emerge compared with bulk material. Another reason is that the nanostructures possess piezoelectric effect, which causes the shift of Raman modes, as the confinement is anisotropic, it has different effect on different phonon

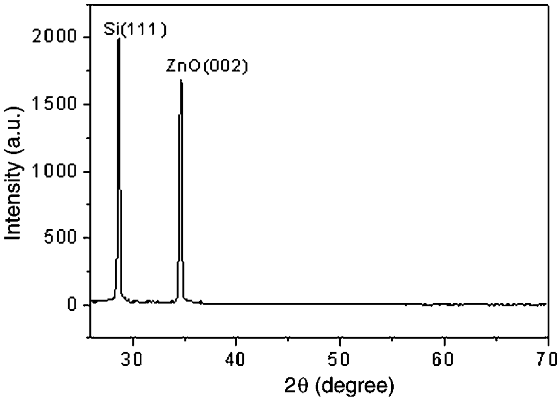

Fig. 2. X-ray pattern of the ZnO nanorod arrays.

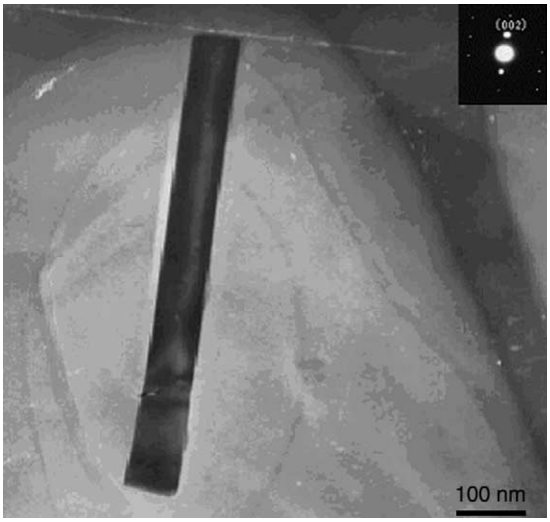

Fig. 3. TEM image of the single ZnO nanorod. The inset is SAED analysis of the nanorod.

modes, as a result the blue shift of E_2 (high) mode and A_1 (LO) mode is different. The peak at 331 cm^{-1} and the broad feature between 1000 and 1200 cm^{-1} can be responsible for the multiphonon processes. These multiphonon processes presumably occur when phonon wave vectors considerably shifted away from the center of the Brillouin zone [21].

The PL spectra of the ZnO nanorods were measured using an He–Cd laser of 325 nm as excitation source. Fig. 5 shows the room-temperature PL spectra of the ZnO nanorods. The spectrum of the as-grown ZnO nanorods mainly consists of a strong UV emission and a very weak deep-level emission. The UV emission, locating at 3.26 eV, is the exciton recombination related near-band edge emission of ZnO and the very weak deep-level emission usually results from the radiative recombination of a photo-generated hole with an electron occupying the oxygen vacancy [22], the UV emission is red-shift compared with that of bulk material. The oxygen vacancies in ZnO can be modified by annealing the samples in O_2 atmosphere [23]. We annealed our sample under O_2 atmosphere at 600, 650 and 850 °C, respectively. The deep-level emission can be totally quenched at 600 °C with a strong UV emission. But when the temperature goes to 650 °C, the deep level emission starts to get higher than that of the as-synthesized sample. When the annealing temperature above 850 °C, the deep-level emission eventually dominants the PL spectrum. We think this behavior is due to the competition between the O atoms getting into the lattice and those evaporating out of the ZnO lattice in O_2 atmosphere. At lower annealing temperature, the kinetic energy of atoms in the ZnO lattice is relatively low and the adsorption rate of the O atoms is faster than the escaping rate. So more O atoms can compensate the O vacancies at lower temperature (<600 °C). But at higher annealing temperatures, the kinetic energy of the atoms becomes larger and larger, possibly resulting in a larger escaping rate of O atoms than the adsorption rate to make more O vacancies in the ZnO lattice. This also strongly suggests that the deep-level emission is the result of oxygen vacancies in the ZnO nanorods. One thing we want to point out is that the observed optimized thermal annealing temperature of 600 °C is much lower than that of 900 °C for ZnO thin films [24]. This will not be a surprise if the much larger reactive surface for ZnO nanorods compared with that of thin films is considered. The UV emission peak of the 600 °C annealing sample is slightly red-shift compared with the as-synthesized one caused by compressive strain formed during the low-temperature growth of the nanorods, when annealed the sample at high temperature, the strain relaxed, which causes the change of the band-gap of the ZnO nanorods. Therefore, from the PL spectra we can find slightly red-shift of the UV emission. When anneal the sample at higher temperatures, the UV emission peaks further red-shift and broaden with increasing annealing

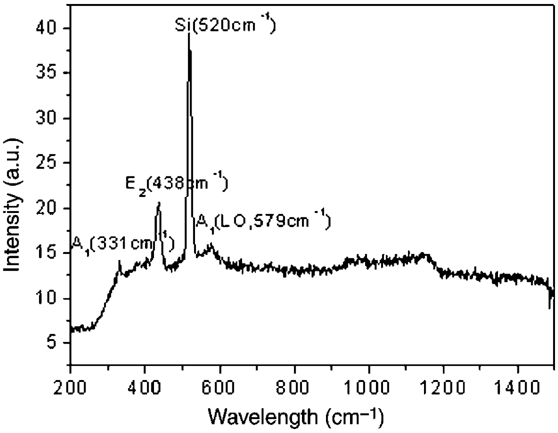

Fig. 4. Raman scattering spectrum of the ZnO nanorod arrays.

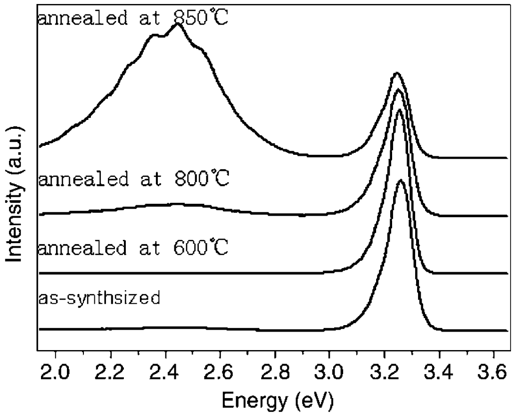

Fig. 5. The room temperature PL spectra of the as-synthesized and thermal annealed samples at different temperatures of the ZnO nanorods.

temperatures, which result from the defect related shallow binding excitons formed during high temperature annealing.

4. Conclusions

In summary, we demonstrated the synthesis of ZnO nanorods arrays by a simple vapor phase transport process. The as-synthesized nanorods have a uniform length of about 1 μm. From the results of XRD, TEM together with the strong UV emission in the PL spectrum, we can find that the obtained ZnO nanorods arrays have good crystal quality and excellent optical properties when the near band-edge emissions are concerned.

Acknowledgements

This work is supported by the '863' High Technology Research Program in China, under Grant No. 2001AA311120, the key Project of National Natural Science Foundation of China under Grant No. 60336020, the Innovation Project of Chinese Academic of Sciences, the National Natural Science Foundation of China under Grant No. 60278031, No. 60176003, and No. 60376009.

References

[1] G.T. Kim, J. Muster, V. Krstic, J.G. Park, Y.W. Park, S. Roth, M. Burghard, Appl. Phys. Lett. 76 (2000) 1875.
[2] N.J. Stone, H. Ahmed, Appl. Phys. Lett. 73 (1998) 2134.
[3] Y. Cui, Q. Wei, H. Park, C.M. Lieber, Science 293 (2001) 1289.
[4] M.H. Huang, S. Mao, H. Feick, H. Yan, Y. Wu, H. Kind, E. Weber, R. Russo, P. Yang, Science 292 (2001) 1897.
[5] H. Chik, J. Liang, S.G. Cloutier, N. Kouklin, J.M. Xu, Appl. Phys. Lett. 84 (2004) 3376.
[6] Y.C. Kong, D.P. Yu, B. Zhang, W. Fang, S.Q. Feng, Appl. Phys. Lett. 78 (2001) 407.
[7] M.H. Huang, Y. Wu, H. Feick, N. Tran, E. Weber, P. Yang, Adv. Mater. (Weinheim, Germany) 13 (2001) 113.
[8] Y.W. Wang, L.D. Zhang, G.Z. Wang, X.S. Peng, Z.Q. Chu, C.H. Liang, J. Cryst. Growth 234 (2002) 171.
[9] H.Z. Zhang, X.C. Sun, R.M. Wang, D.P. Yu, J. Cryst. Growth 269 (2004) 464.
[10] J.J. Wu, S.C. Liu, J. Phys. Chem. B 106 (2002) 9546.
[11] J.-J. Wu, S.-C. Liu, Adv. Mater. 14 (2002) 215.
[12] X.M. Sun, X. Chen, Z.X. Deng, Y.D. Li, Mater. Chem. Phys. 78 (2002) 99.
[13] L. Vayssieres, Adv. Mater. 15 (2003) 464.
[14] C.-H. Hung, W.-F. Whang, Mater. Chem. Phys. 82 (2003) 705.
[15] W.I. Park, G.-C. Yi, J.-W. Kim, S.-M. Park, Appl. Phys. Lett. 82 (2003) 4358.
[16] W.I. Park, G.-C. Yi, M. Kim, S.J. Pennycook, Adv. Mater. 15 (2003) 526.
[17] W.I. Park, G.C. Yi, Adv. Mater. 16 (2004) 87.
[18] S.W. Jung, W.I. Park, G.-C. Yi, M. Kim, Adv. Mater. 15 (2003) 1358.
[19] S.C. Lyu, Y. Zhang, C.J. Lee, H. Ruh, H.J. Lee, Chem. Mater. 15 (2003) 3249.
[20] X.T. Zhang, Z. Liu, Y.P. Leung, Q. Li, S.K. Hark, Appl. Phys. Lett. 83 (2003) 5533.
[21] T.C. Damen, S.P.S. Porto, B. Tell, Phys. Rev. 142 (1966) 570.
[22] K. Vanheusden, W.L. Warren, C.H. Sesger, D.R. Tallant, J.A. Voigt, B.E. Gnage, J. Appl. Phys. 79 (1996) 7983.
[23] J. Lim, K. Shin, H.W. Kim, C. Lee, Mater. Sci. Eng. B 107 (2004) 301.
[24] Z.Z. Zhi, Y.C. Liu, B.S. Li, X.T. Zhang, Y.M. Lu, D.Z. Shen, X.W. Fan, J. Phys. D 36 (2003) 719.